CONF-9105220--1

DE91 014572

GRAPHITE FOR THE NUCLEAR INDUSTRY

T. D. Burchell, E. L. Fuller, G. R. Romanoski and J. P. Strizak

Oak Ridge National Laboratory, Oak Ridge, Tennessee 37831-6088, USA.

1.0 Introduction

Graphite finds applications in both fission and fusion reactors. Fission reactors harness the energy liberated when heavy elements, such as uranium or plutonium, fragment or "fission". Reactors of this type have existed for nearly 50 years. The first nuclear fission reactor, Chicago Pile No. 1, was constructed of graphite under a football stand at Stagg Field, University of Chicago. Fusion energy devices will produce power by utilizing the energy produced when isotopes of the element hydrogen are fused together to form helium, the same reaction that powers our sun. The role of graphite is very different in these two reactor systems. Here we summarize the function of the graphite in fission and fusion reactors, detailing the reasons for their selection and discussing some of the challenges associated with their application in nuclear fission and fusion reactors.

2.0 Fission Reactor Applications

2.1 The Fission Reaction

Nuclear fission reactors utilizes the energy liberated during a controlled fission reaction. The fission reaction may be written:

$$^{235}U + \text{thermal neutron} \rightarrow \text{fission products} + \text{fast neutrons} + \text{energy}.$$

The neutrons produced by a fission reactions are termed "fast" neutrons and typically posses energies in the range 1-10 MeV. Fast neutrons must dissipate most of their energy before they can fission further ^{235}U atoms. Indeed, their energy has to be reduced to thermal levels, typically less

---

This research was sponsored by the Office of New Production Reactors, and the Office of Fusion Energy, U.S. Department of Energy, under contract DE-AC05-84OR21400 with Martin Marietta Energy Systems Inc.

DISCLAIMER

than 0.1 eV. The process of thermalization is achieved through atomic collisions and interactions between the fast neutrons and a "moderator" material, usually a light element, such as water or carbon. Graphite is a convenient form of carbon for fission reactor moderator applications. It is readily available, relatively inexpensive, can be easily machined into complex geometries, and offers sufficient strength to be used in core structural applications.

2.2 Graphite Moderated Gas-Cooled Reactors

The first commercial gas-cooled graphite moderated power generating reactors were the "Magnox" reactors built in the UK[1]. These reactors utilized CO_2 gas as their coolant and the cores were constructed from stacks of radially-keyed PGA graphite blocks. Magnox reactors were also constructed in France, Italy and Japan. The British followed the Magnox reactor with a second generation reactor, known as the Advanced Gas-Cooled Reactor (AGR). AGR reactors were also CO_2 cooled, but had a considerably higher coolant gas outlet temperature (650°C compared to 360°C for the magnox reactor), thereby increasing their efficiency. During the late sixties and early seventies attention turned to the high temperature reactor concept. In these reactors, e.g. Peach Bottom in the USA, AVR in Germany and the Dragon Reactor in the UK (Fig. 1), helium coolant gas was employed for the first time. In the USA a commercial high temperature reactor was built for the Public Service Company of Colorado at Fort St. Vrain, Colorado, by General Atomics, San Diego, California. Currently the USA, Germany and Japan have active gas-cooled reactor research programs. Moreover, the Japan Atomic Energy Research Institute has a High Temperature Engineering Test Reactor (HTTR) under construction at Tokai-Mura. In the USA, the Department of Energy is sponsoring the design of a Modular High-Temperature Gas-Cooled Reactor (MHTGR).

2.3 The Modular High-Temperature Gas-Cooled Reactor

The MHTGR uses graphite both as the moderator and reactor core structural material. The core comprises an array of hexagonal graphite blocks, surrounded by a ring of graphite permanent reflectors (Fig. 2). The fuel particles, which comprise a uranium oxy-carbide kernel coated with silicon carbide and pyrolitic graphite, are mixed with a pitch binder and formed into fuel sticks.

The fuel is loaded into holes running the length of the fuel element (Fig. 3). Each fuel hole is surrounded by coolant gas holes through which the helium coolant flows. The fuel elements are confined to an annular segment in the core (Fig. 4). The coolant flows down through the annular core to the core support region where it mixes and flows out of the core through the cross-duct to the steam generator. Having given up its heat the coolant reenters the core through the cross-duct, flows up and around the outside of the graphite core, thus cooling the metallic pressure vessel, and reenters the annular graphite core at the top of the reactor. Fuel elements and replaceable reflectors are supported on graphite core support posts (Fig. 5). Thus the major components of the reactor core, i.e., fuel element and replaceable reflectors, permanent reflectors, and core support posts, serve different functions and have varying property requirements.
A four module NPR-MHTGR, currently being designed be CEGA Corp., San Diego, California, requires an estimated 34,700 tons of graphite over its forty year life.

2.3.1 MHTGR Graphite Components Property Requirements

2.3.1.1. Fuel Element and Replaceable Reflector

These components endure the highest lifetime neutron fluence, typically up to $5x10^{25}$ n/m^2 [E>0.18 MeV]. Irradiation induced dimensional changes must be isotropic or near isotropic to minimize radiation induced stresses. Near isotropic grades of nuclear graphite were developed in the seventies for the AGR and HTGR programs. In the USA, Great Lakes Carbon Corporation developed their grade H-451, based on near-isotropic petroleum cokes. The irradiation induced dimensional changes of H-451 are compared to those of the anisotropic grade H-327 in Fig. 6. Clearly the near-isotropic grade exhibits much lower dimensional changes. Other desirable properties of fuel element and replaceable reflector graphites include: low coefficient of thermal expansion and high thermal conductivity (to minimize thermal stresses), and toughness or flaw tolerance. Chemical purity is important for several reasons. Firstly, certain elements (e.g. iron, calcium, vanadium) act as catalysts to the graphite-steam reaction. Secondly, elements such as chromium, cobalt and europium activate and create handling problems after discharge from the reactor. Lastly, certain elements, particularly boron, have a very high neutron capture cross section and thus give rise to unacceptably high parasitic neutron losses.

2.3.1.2. Permanent Reflectors

The permanent reflectors are large components, requiring graphite billets up to 50 inches in diameter. They are subject to a relatively low neutron fluence and thus do not need to be near-isotropic. Permanent reflectors are not highly stressed. High chemical purity is required for the reasons stated above. The graphite selected for this application must be available in large sizes at reasonable cost.

2.3.1.3. Core Support Posts

Core support posts must posses adequate strength to support the core, and sustain transient thermal and seismic stresses. High strength is a particularly desirable property in the graphite used for this component. These components are designed for a forty year life. Oxidation induced strength loss must be minimized and therefore high chemical purity is a stringent requirement[2].

2.4 The Effect of Reactor Environment on Graphite Properties.

2.4.1 Temperature

Many properties of graphite are influenced by temperature. The strength, elastic moduli, coefficient of thermal expansion and specific heat all increase with increasing temperature. Thermal conductivity decreases as temperature increases. Perhaps one of the most significant effects of increasing temperature is an acceleration of graphite air and steam oxidation.

2.4.2 Helium Coolant Gas

The helium carries trace amounts of air and water-vapor. These are responsible for gasification (oxidation) of the graphite. Oxidation reduces strength, moduli, and thermal conductivity.

2.4.3 Neutron Irradiation.

Neutron irradiation causes volume and dimensional changes to occur in the graphite[3-5]. The basic mechanism of neutron damage is shown in Figure 7. Fast neutron collisions cause the displacement of carbon atoms from their lattice sites. These primary atoms may in turn displace other, secondary atoms. Indeed, approximately 1,000 carbon atoms are displaced by a 2 MeV neutron. The displaced carbon atoms tend to aggregate between the graphite crystal basal planes, forming new layer planes or, depending upon the temperature, may migrate and recombine with vacant sites. The formation of new planes causes a swelling in the crystallographic c-direction, while the displacement of carbon atoms from the basal planes result in an a-direction shrinkage. Initially the c-direction swelling is accommodated by internal voids which tends to be preferentially aligned between the crystal basal planes. Thus the bulk materials behavior is dominated by the a-direction shrinkage and the graphite densifies (volumetric shrinkage). This is shown schematically in Figure 8. With continued irradiation the accommodating voids are filled and the graphite begins to undergo bulk expansion. This phenomena, known as "turnaround" occurs at lower fluences for higher irradiation temperatures (Fig. 8). This is attributable to the increasing amount of accommodating voidage filled at higher temperatures by internal thermal expansion. Eventually, c-direction swelling of the crystallites causes boundary shearing and internal cracking of the graphite, resulting in structural and property deterioration. Dimensional change data for grade H-451 in the with-grain (parallel to extrusion direction), at two irradiation temperatures, 600 and 900°C, are shown in Figure 9.

Neutron damage of the graphite crystal lattice has other significant effects on physical properties. Basal plane dislocations are pinned at vacancies, thus causing an increase in strength and elastic moduli. However both strength and moduli diminish after the "turnaround" fluence is exceeded. The closure of accommodating voidage increases the coefficient of thermal expansion. Irradiation induced crystallographic defects act as phonon scattering centers, decreasing thermal conductivity.

Thermal creep in graphite becomes significant only at temperatures in excess of 2000°C. However, under neutron irradiation, creep occurs at much lower temperatures. Thus the thermal and irradiation induced strains in reactor components creep out, alleviating the risk of premature failure

of the components. During reactor cooldown thermal stresses will reappear, but in the opposite direction.

3.0 Fusion Device Applications

3.1 The Fusion Reaction

The fusion reaction, shown schematically in Figure 10, involves bringing together and "fusing" two isotopes of hydrogen at very high temperatures. The two isotopes are deuterium, consisting of one proton and one neutron, and tritium, which consists of one proton and two neutrons. When deuterium and tritium fuse the element helium (two protons and two neutrons) is formed and one highly energetic neutron (14.1 MeV) is liberated. The reaction may be written:

$$^{2}H + {}^{3}H \rightarrow {}^{4}He + {}^{1}n \ (14.1 \text{ MeV}).$$

Controlled nuclear fusion is obtained by magnetically confining a gaseous plasma of deuterium and tritium and heating it by the passage of electric current, neutral beam injection and microwave excitation. A plasma core temperature of hundreds of millions of degrees celsius is required to achieve fusion. The experimental device most commonly used to study fusion is the "tokamak". However, to date tokamaks have not been able to achieve the required combination of sufficiently high plasma temperatures and long plasma confinement times to attain controlled nuclear fusion. The essential features of a tokamak are a torus-shaped (doughnut) vacuum vessel, toroidal and poloidal magnetic coils, plasma heating and diagnostics. The inner surface of the vacuum vessel must be protected from the plasma because fusion plasmas cannot tolerate high-atomic number impurities, such as the alloys typically used for the vacuum vessel. Consequently, another essential feature of a tokamak is a low atomic number armor material (typically graphite) that faces the plasma.

3.2 Experimental Tokamak Fusion Reactors

Several large tokamak devices exist worldwide and are used to study the physics of plasma fusion[6]. These include the Tokamak Fusion Test Reactor (TFTR) at Princeton University, USA; General Atomic's DIIID at San Diego, California; the Joint European Torus (JET) at Culham, UK; Tore

Supra, France; and, JT-60U in Japan. Three "next generation" large experimental tokamak fusion reactors are currently being designed: The Burning Plasma Experiment (BPX) is planned for the Princeton Plasma Physics Laboratory; the Next European Torus (NET) is being planned by the European states; and, the International Thermo-Nuclear Experimental Reactor (ITER), which is being designed by an international team from the USA, USSR, Japan and Europe. The ITER project is the most ambitious fusion reactor project to date. It is most certainly the largest device of its kind ever considered. Figure 11 shows a section through the ITER vacuum vessel. Plasma facing components called "divertors" are located at the top and bottom of the vessel. The function of the divertor is to divert energetic particles that escape from the plasma edge away from the vessel wall and out through the exhaust duct. The inboard and outboard surfaces of the vessel are protected with plasma facing components (shown hatched in Fig. 11). When the plasma disrupts, the divertors and other plasma facing components are subject to extremely high heat fluxes. Consequently, thermal shock resistance and high thermal conductivity (to minimize the surface temperature) are desirable materials properties. Other attractive properties of plasma-facing materials include: low atomic number (to minimize radiative heat losses from the plasma impurities), erosion resistance (plasma sputtering), and adequate strength and stiffness. In ignition machines (i.e., ones that sustain a D-T fusion plasma) a plasma facing material property of considerable significance will be neutron damage resistance.

3.3 Graphite and Carbon-Carbon Composites as Plasma Facing Components

Graphite has been used as a plasma facing component in several experimental tokamaks[7,8]. It possesses many of the attributes discussed previously. More recently devices such as TFTR and JT-60U have switched to carbon-carbon composites because of their enhanced thermal shock resistance and superior mechanical properties. Next generation machines, such as ITER, will require the high thermal conductivities offered by carbon-carbon composites to manage the enormous heat loads their plasma facing components will be subjected to.

One particularly attractive feature of carbon-carbon composites is their "tailorability". The material may be engineered to give the desired properties through appropriate selection of fiber type, fiber distributions, architecture and processing. A schematic of a three-directional carbon-carbon

composite is shown in Figure 12. The fibers used in the manufacture of carbon-carbon composites are made from rayon, Polyacrylonitrile (PAN) or pitch precursors. Pitch fibers, which posses the greatest thermal conductivities, currently as high as 1300 W/m•K, are manufactured in the USA from oil-derived mesophase pitches.

3.4 Radiation Damage in Carbon-Carbon Composites

In addition to damage from the 14.1 MeV fusion neutrons, first wall graphite and carbon-carbon composites under irradiation in a fusion spectrum will undergo the reactions,

$$^{12}C(n, \alpha)^{9}Be \text{ and } ^{12}C(n, n')3\alpha,$$

both of which produce damage in graphites and carbon-carbon composites in excess of the pure neutron displacement damage. The basic mechanism of radiation damage in graphites is well understood and is described in section 2.4.3. In attempting to predict the irradiation response of carbon-carbon composites we must first understand the behavior of carbon fibers.

The basic mechanism of radiation damage in carbon fibers is identical to that of graphites and may be interpreted through a microstructural model such as in Fig. 13. The crystallographic layer planes are modelled as a core-sheath arrangement, with the c-direction radial and the two a-directions circumferential and axial. We expect a-direction shrinkage and c-direction growth to occur. However, just as in the case of bulk graphites c-axis growth is accommodated by interplaner voids, and initially we only observe the a-axis shrinkage. This causes the fiber to shrink both axially and diametrically, and at higher fluences to expand diametrically while continuing to shrink axially. Ultimately the fiber will develop radial cracks (Fig. 14) which are attributed to the combination of circumferential shrinkage and radial expansion. This behavior is consistent with previous data of Gray[9] and Price et al[10]. Fibers with a density close to theoretical, i.e., >2.0 g/cm^3, would not be expected to exhibit diametrical shrinkage because of the limited amount of accommodating internal voids.

The axial shrinkage of the carbon fiber dominates the behavior of carbon-carbon composites. For 2D materials such as those shown in Fig. 15 the response of the material to irradiation damage will depend on the orientation of the woven fiber layers. The fiber axial shrinkage will result in a radial shrinkage for specimens of the type shown in case II of Fig. 15. Moreover, the associated increase in the woven-fabrics crimp will result in an expansion along the specimens axis. If the fabric utilizes an unbalanced weave the specimen will tend to become oval during irradiation.

In their study Price et al[10]. demonstrated the superior performance of pitch fibers compared with that of PAN fibers under identical irradiation conditions. Their results are attributable to the increased crystallinity of pitch fibers compared to PAN fibers. This results in lower irradiation-defect concentrations in pitch fiber crystallites because the probability of interstitial-vacancy pair recombination is increased. A comparison of the behavior of two-directional (2D) carbon-carbon composite materials of similar architectures (Table 1), suggests the superior performance of the pitch fiber may be translated to the composite material.

Table 1. Dimensional Changes of 2D Carbon-Carbon Composites Irradiated at 400°C.

ID	Fiber	Fluence (dpa)*	Dimensional Changes (%) Thickness	Diameter
CC-1	Pitch	12.3	24.4	-9.2
CC-2	Pitch	12.1	22.8	-9.7
CC-3	PAN	11.5	33.1	-5.8/-18.8
CC-4	PAN	11.4	36.9	-3.0/-17.7

* Displacements per atom.

4.0 Coal Derived Products for the Nuclear Industry

As discussed above, carbon and graphite products play vital roles in fission and fusion reactors. At the present time US nuclear grade graphites are made from near-isotropic petroleum cokes. Moreover, high-conductivity pitch fibers of the type required for fusion energy applications are manufactured from petroleum mesophase pitch. Evidently, the US carbon product industry is dependent upon the petroleum industry for its raw materials.

Other countries, notably Japan and Germany, have developed isotropic cokes from coal-tar pitches. Moreover, Mitsubishi Kaisi (Japan) manufactures high-conductivity carbon fibers derived from coal-tar pitches. Coal-tar pitch is a by-product of the conversion of coal to metallurgical coke. However, the recent trend toward direct reduction of iron, the increasing popularity of beehive kilns, and the environmental problems associated with the operation of metallurgical coke ovens, have cast doubt over the long term availability of coal tar pitches. This is a serious concern in the graphite industry, since the preferred binder material for graphite manufacture is coal tar pitch.

If coal-derived pitches, cokes and fibers are to be adopted in the USA it would appear that a necessary first step is the development of a clean and reliable pitch extraction process. Having first achieved this, efforts should then be turned toward coal selection, and/or feedstock (extract) modification, to produce pitches optimized for the manufacture of isotropic cokes or high-conductivity pitch fibers. Finally, the development of near-isotropic nuclear graphites from coal-derived isotropic cokes is encouraged.

5.0 Conclusions

Nuclear applications of graphite have been reviewed. The current dependence of the US industry on petroleum derived precursors has been highlighted. The desirability of an alternative coal tar pitch extraction method is noted and some research directions are recommended.

6.0 References

1. N. Prince. Technology of graphite moderator structures, Nuclear Energy, Vol. 18, No. 4, pp. 267-275, 1979.

2. R. A. Strehlow and H. C. Young. ORNL/GCR-84/6, Summary of Results of Test Zero, Phase Two of the Core Support Performance Test Series, August 1984. Oak Ridge National Laboratory.

3. R. E. Nightinale. Nuclear Graphites, Academic Press, New York, 1962.

4. J. H. W. Simmons. Radiation Damage in Graphite, Pergamon Press, 1965.

5. B. T. Kelly. Physics of Graphite, Applied Science Publishers, 1981.

6. J. Sheffield. Magnetic Fusion Progress: A History and Review, ORNL Review, No. 4, 1987. Pub. Oak Ridge National Laboratory.

7. G.B. Engle and B. T. Kelly. Radiation Damage of Graphite in Fission and Fusion Reactor Systems, J Nucl. Mater., Vol. 122 & 123, p. 122, 1984.

8. W. P. Eatherly, R. E. Clausing, R. A. Strehlow, C. R. Kennedy and P. K. Mioduszewski. ORNL/TM-10280, Graphite for Fusion Energy Applications. Oak Ridge National Laboratorty. March 1987.

9. W. J. Gray. BNWL-2390, Neutron Irradiation Effects on Carbon and Graphite Cloths and Fibers. Battelle Pacific Northwest Laboratories. August 1977.

10. R. J. Price, R. J. Hopkins and G. B. Engle. *Proceedings of 17th Biennial Conference on Carbon,* p. 340, 1985.

Figure captions

Figure 1. Schematic diagram of the DRAGON reactor at Winfrith, UK.

Figure 2. Cross-section through the MHTGR Core showing annular fuel region and replaceable and permanent reflectors.

Figure 3. Schematic diagram of a typical MHTGR fuel element.

Figure 4. Graphite reactor internals of the MHTGR.

Figure 5. Schematic diagram of the MHTGR graphite core support structure.

Figure 6. Comparison of the dimensional changes of graphite grades H-327 and H-451/H-429

Figure 7. Mechanism of radiation damage in graphite.

Figure 8. Schematic diagram of the irradiation induced dimensional changes of graphite at various temperatures.

Figure 9. Radiation induced dimensional changes in graphite grade H-451.

Figure 10. Schematic illustration of the ^{2}H-^{3}H fusion reaction.

Figure 11. Schematic illustration of a cross-section through the ITER vacuum vessel.

Figure 12. Illustration of a three-directional orthogonal carbon-carbon composite.

Figure 13. Schematic illustration of radiation damage in carbon fibers.

Figure 14. Schematic illustration showing development of irradiation induced fiber voids and cracks.

Figure 15. Schematic illustration of irradiation induced dimensional changes in two-dimensional carbon-carbon composite specimens.

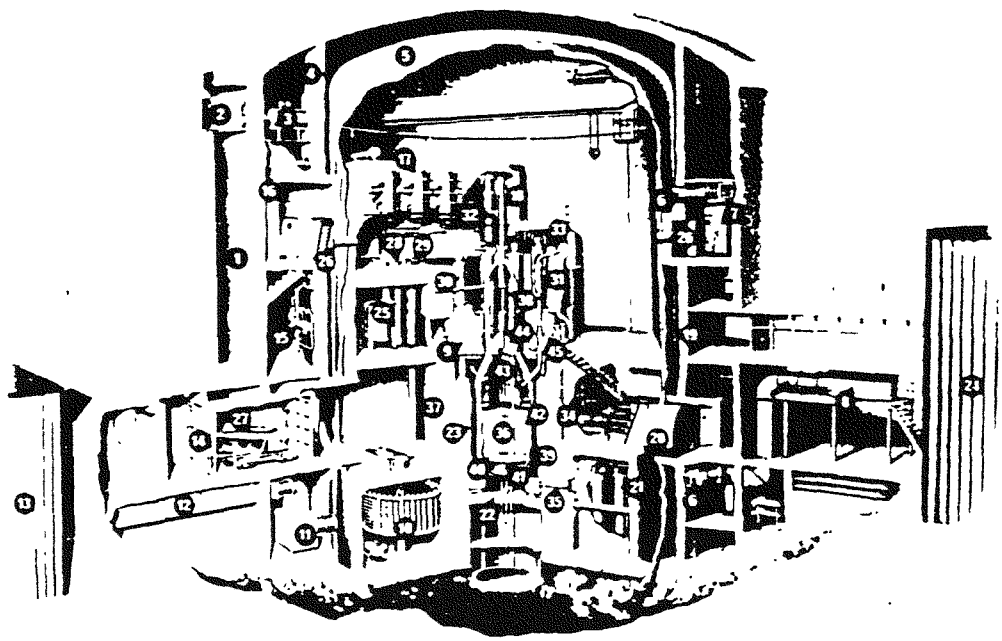

1 Outer Concrete Containment
2 Shut Down Coolers
3 Water Storage Tanks
4 Inner Concrete Wall
5 Inner Containment Steel Shell
6 Circulating Ventilation Plant
7 Crane Control Room
8 Main Ventilation Inlet & Filters
9 Loose Shield Blocks
10 Fuel Element Storage Roundabout
11 Ventilation Exhaust Filters
12 Ventilation Exhaust to Stack
13 Active Storage Block
14 Vehicle Air Lock Entrance
15 Secondary Coolant Control Valve
16 Charge Machine Control Room
17 Secondary Heat Exchangers
18 Charge Machine
19 Personnel Air Lock Access
20 Emergency Air Lock Access
21 Helium Delay Beds
22 Bottom Biological Shield
23 Steel-Water Thermal Shield
24 Control Block
25 Secondary Coolant Dump Tank
26 Observation Windows
27 Transit Flask
28 Fuel Element Charge Chute
29 Fuel Element Discharge Chute
30 Canning Cell
31 Primary Heat Exchangers
32 Load Facility Transfer Flask
33 Primary Circulator
34 Compressor Room
35 Ion Chambers
36 Core
37 Neutron Shields
38 Seal Bung
39 Main Pressure Vessel
40 Core Bed Plate
41 Fission Product Pipes
42 Reflector
43 Absorber Rods
44 Main Shield Plug
45 Thermocouple (Helium Temp.)

Figure 1. Schematic diagram of the DRAGON reactor at Winfrith, UK.

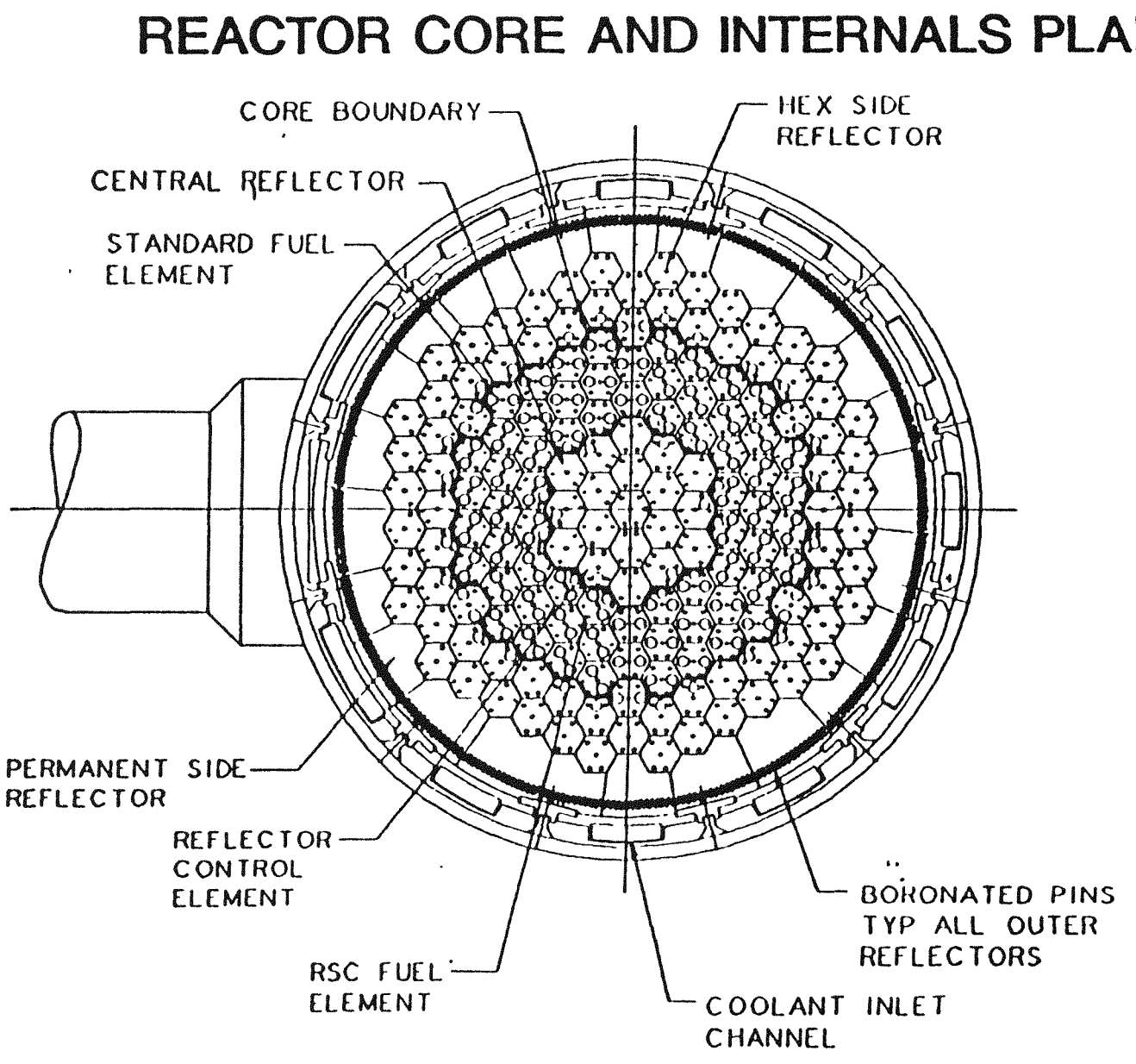

Figure 2. Cross-section through the MHTGR Core showing annular fuel region and replaceable and permanent reflectors.

ORNL-DWG 91M-5888

TYPICAL NP-MHTGR GRAPHITE CORE COMPONENT
(FUEL/TARGET ELEMENT)

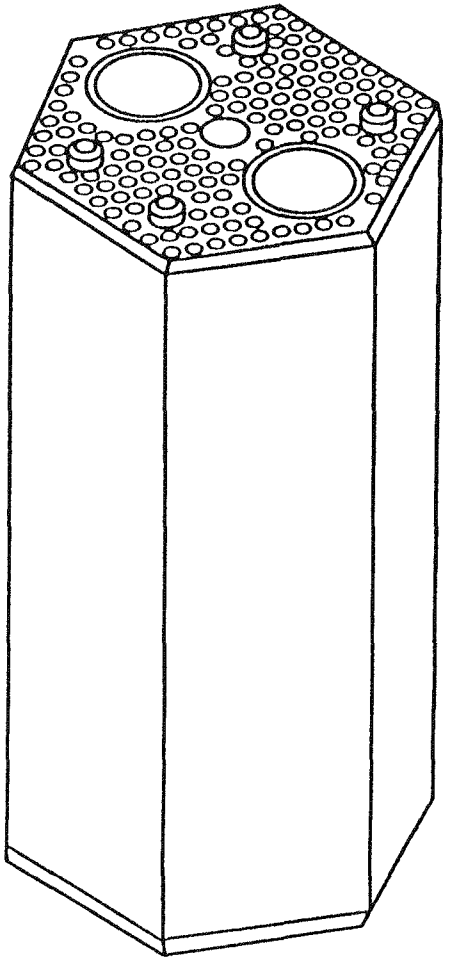

Figure 3. Schematic diagram of a typical MHTGR fuel element.

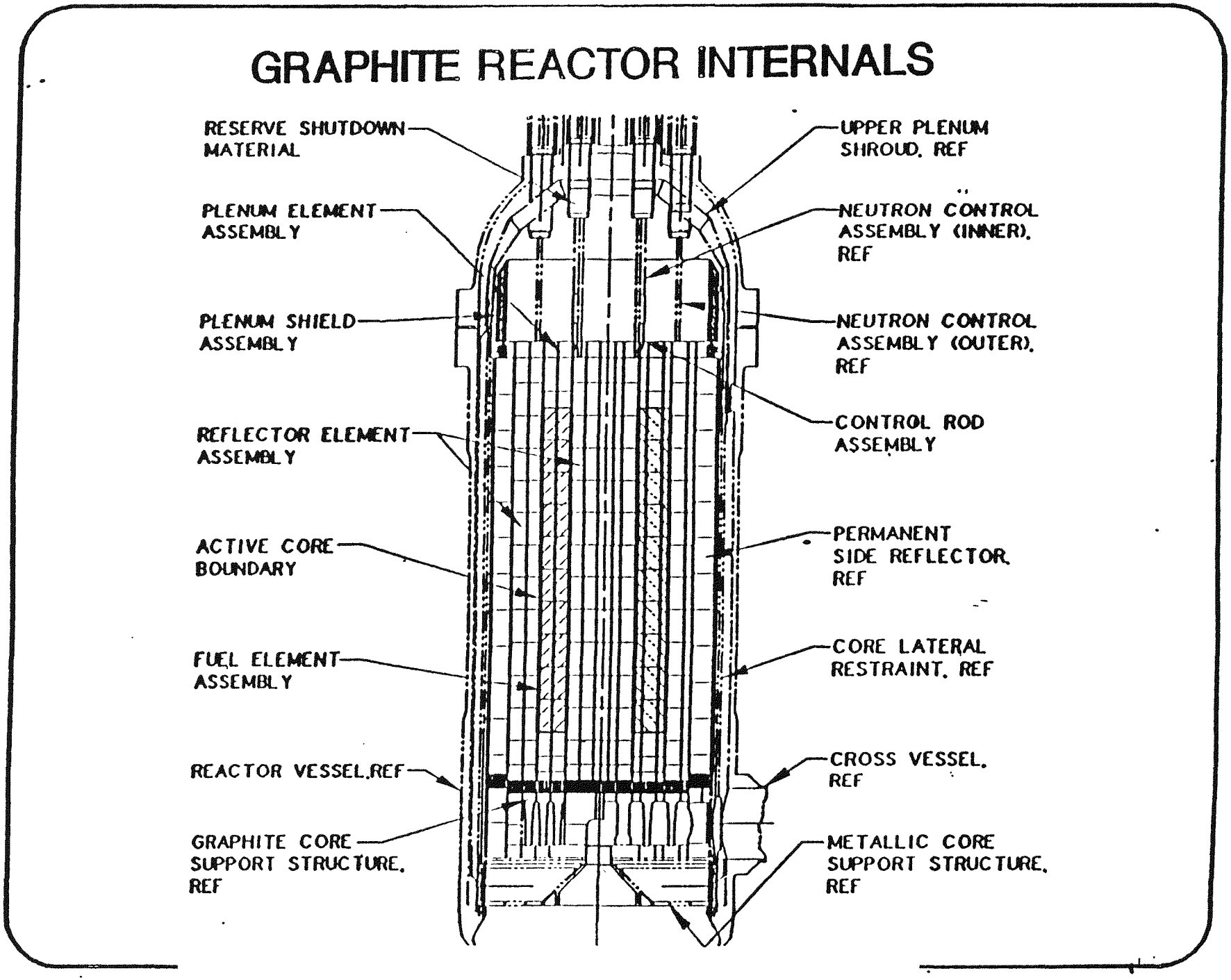

Figure 4. Graphite reactor internals of the MHTGR.

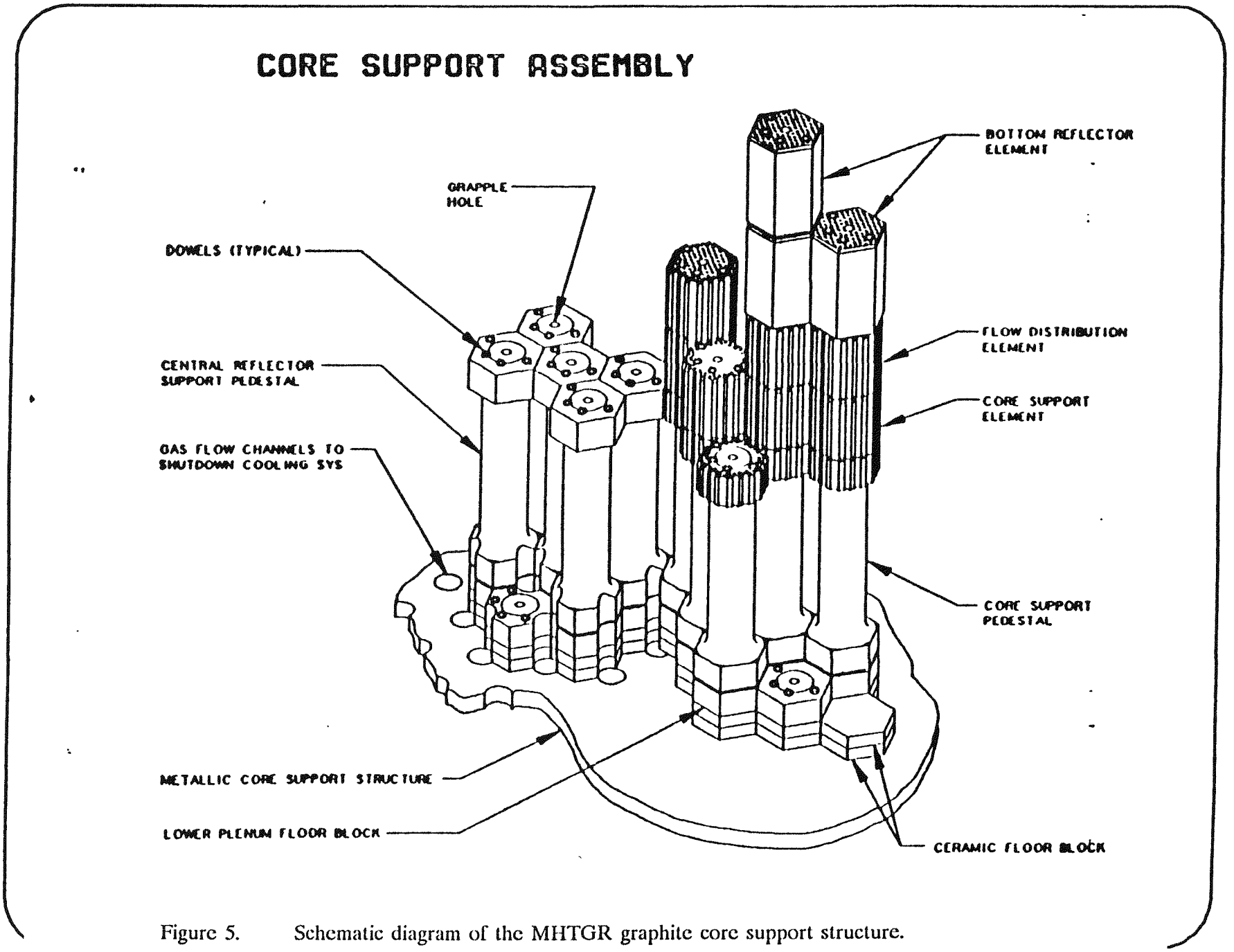

Figure 5. Schematic diagram of the MHTGR graphite core support structure.

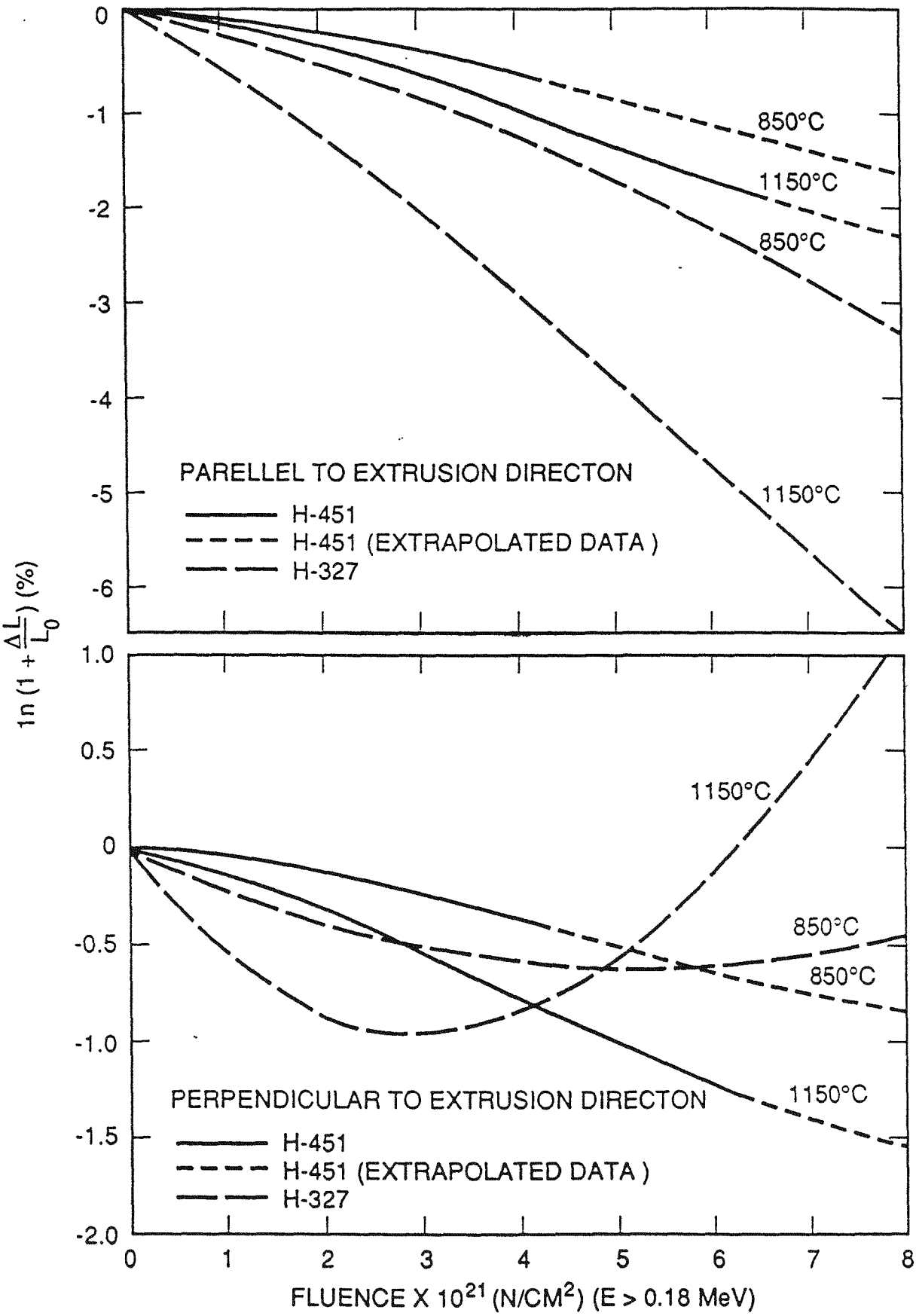

Figure 6. Comparison of the dimensional changes of graphite grades H-327 and H-451/H-429

RADIATION DAMAGE IN GRAPHITE

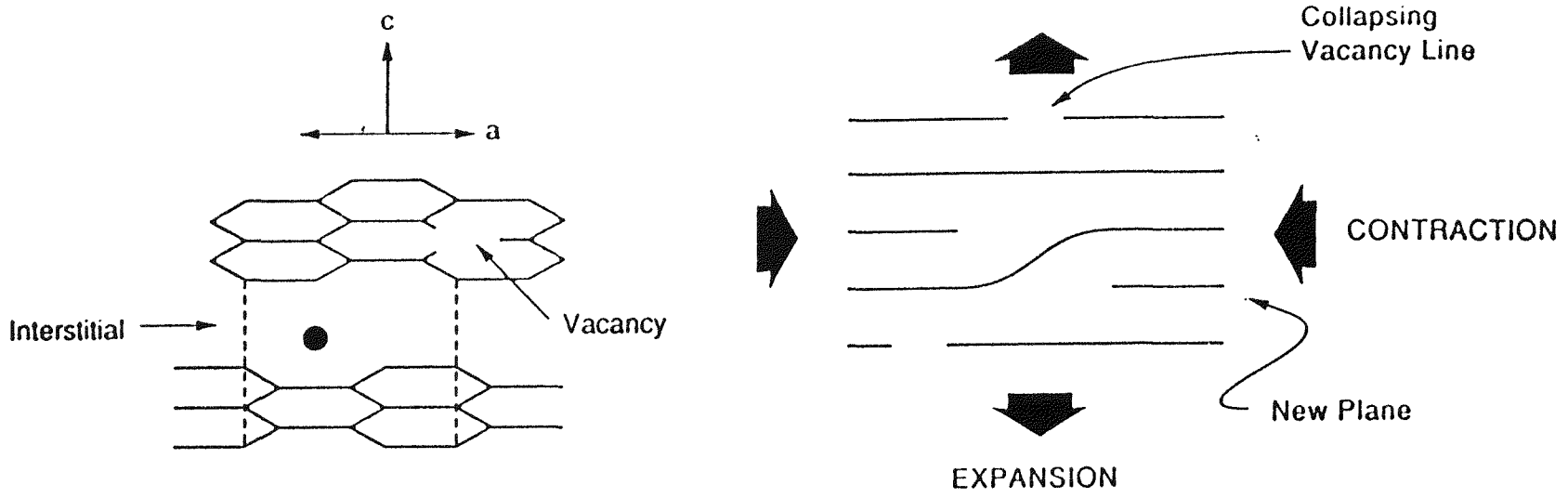

Radiation damage in graphite arises from neutron displacement of carbon atoms, creating a vacancy-interstitial pair.

At the temperatures of interest, vaccancies collapse and are swept out of the graphite crystal, resulting in shrinkage of the planes (a-direction). Interstitials aggregrate to form new planes thus causing a swelling in the c-direction.

Nuclear - type polycrystalline bulk graphites are specially fabricated to be isotropic on a microscopic scale and posses a void texture to accomodate much of the crystallite swelling.

ornl

Figure 7. Mechanism of radiation damage in graphite.

ORNL-DWG 88-14208

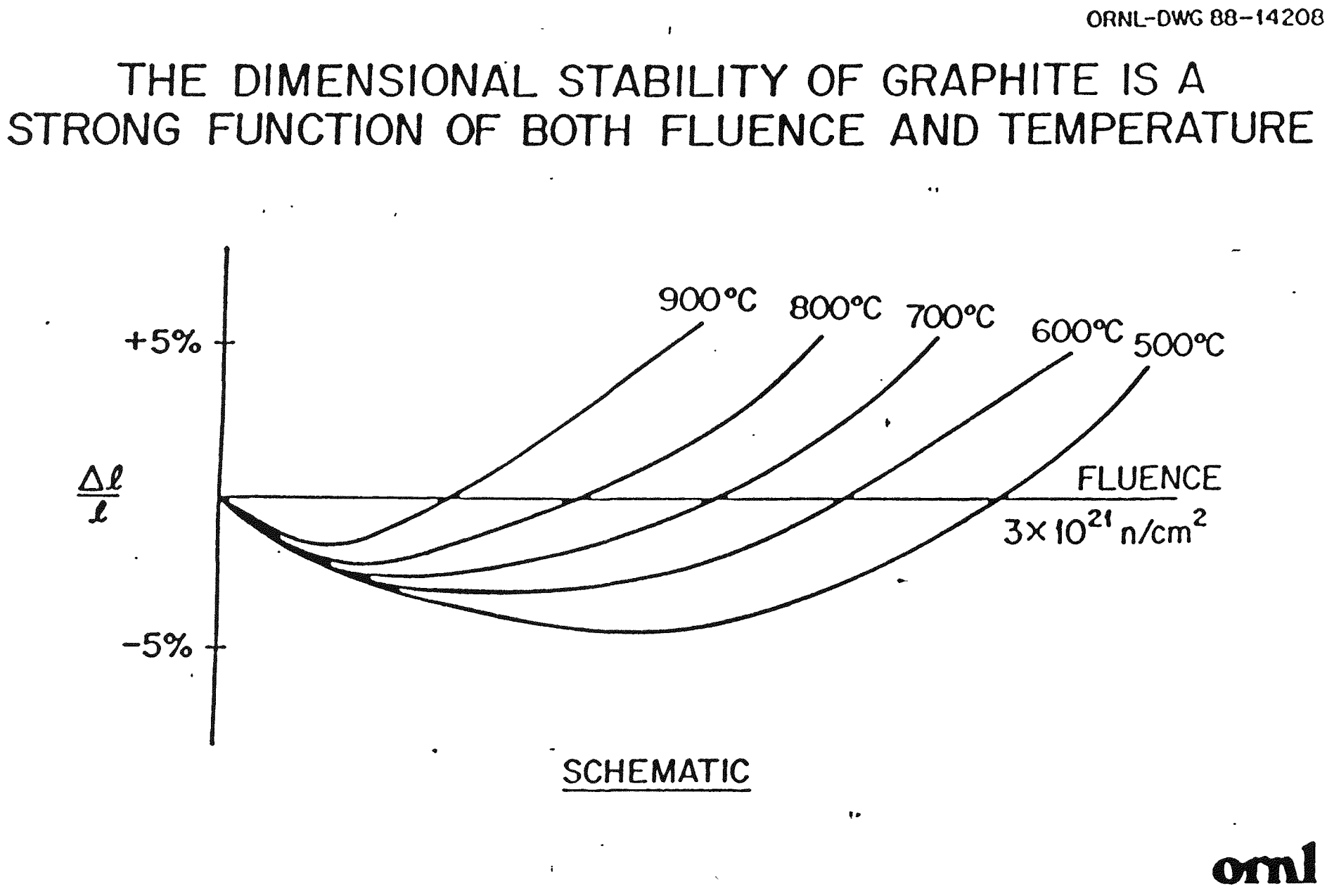

Figure 8. Schematic diagram of the irradiation induced dimensional changes of graphite at various temperatures.

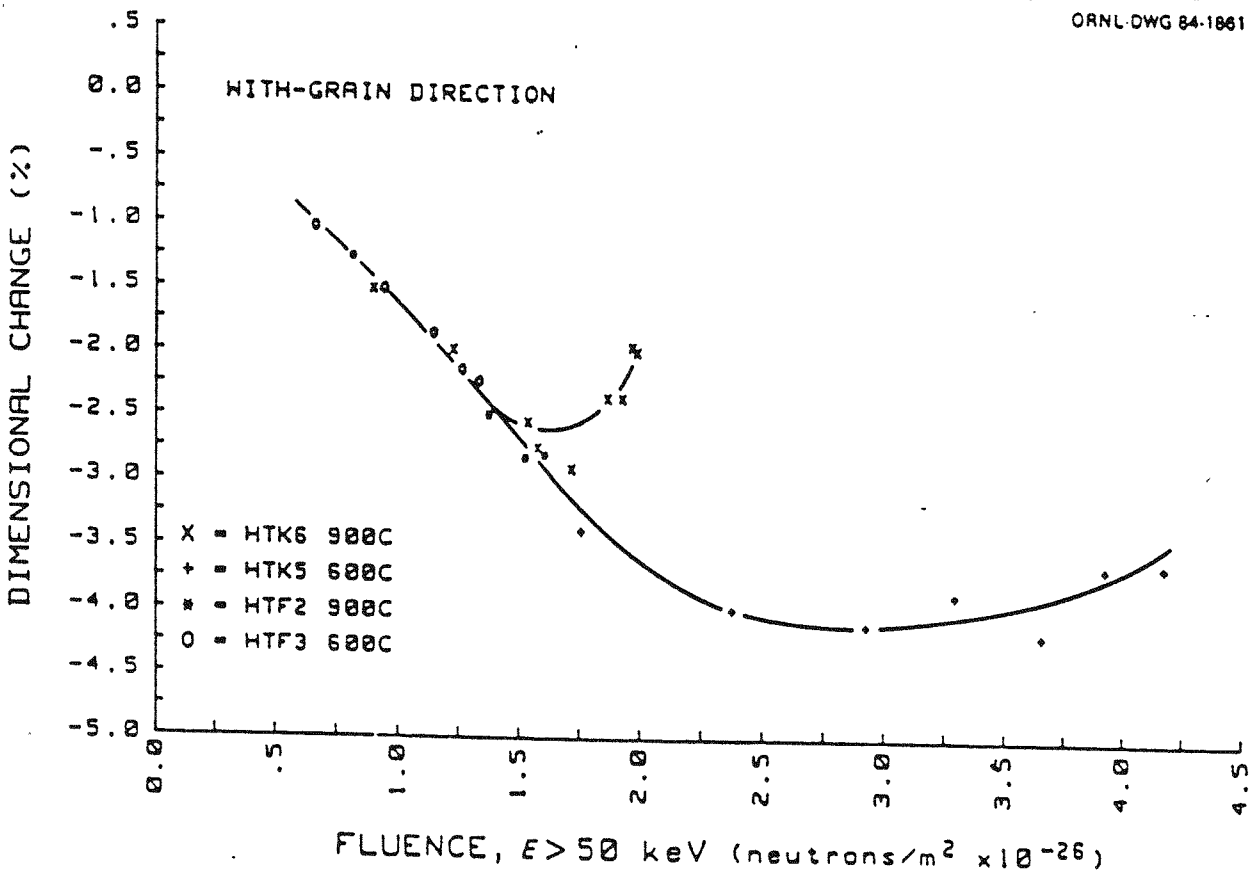

Figure 9. Radiation induced dimensional changes in graphite grade H-451.

ornl

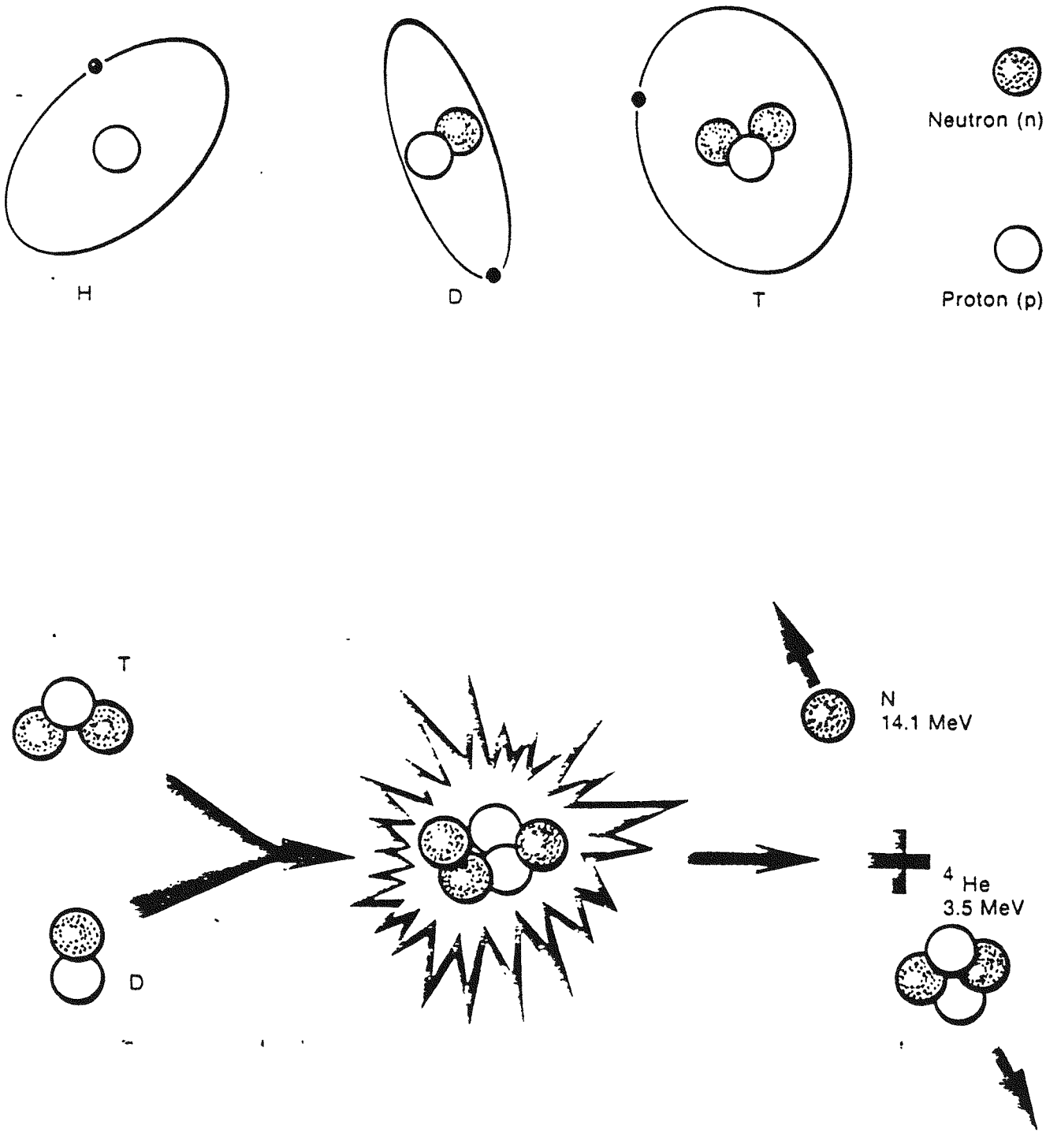

Figure 10. Schematic illustration of the ^{2}H-^{3}H fusion reaction.

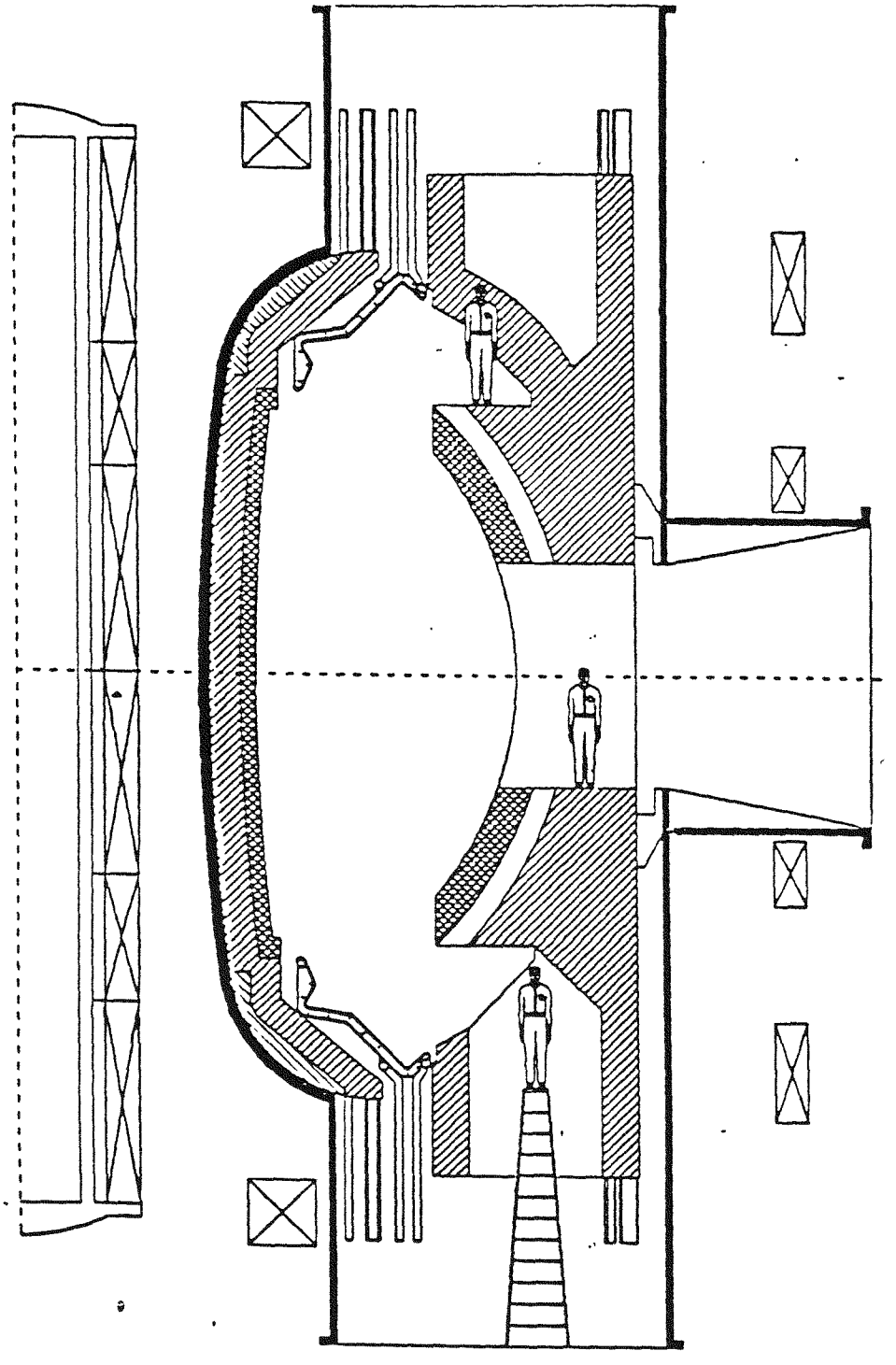

Figure 11. Schematic illustration of a cross-section through the ITER vacuum vessel.

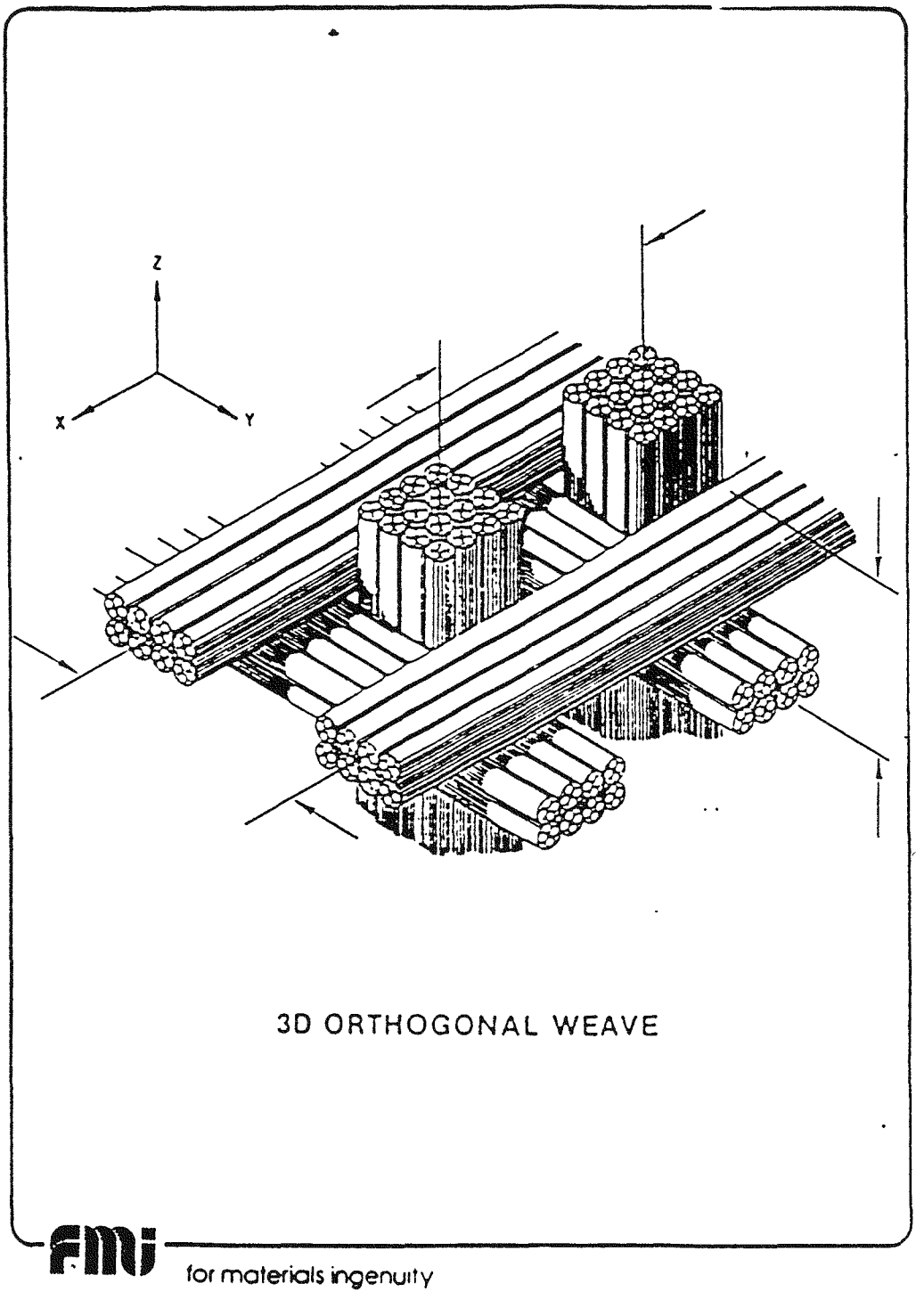

Figure 12. Illustration of a three-directional orthogonal carbon-carbon composite.

RADIATION DAMAGE IN CARBON FIBERS

- ***Simplified fiber microstructure:***

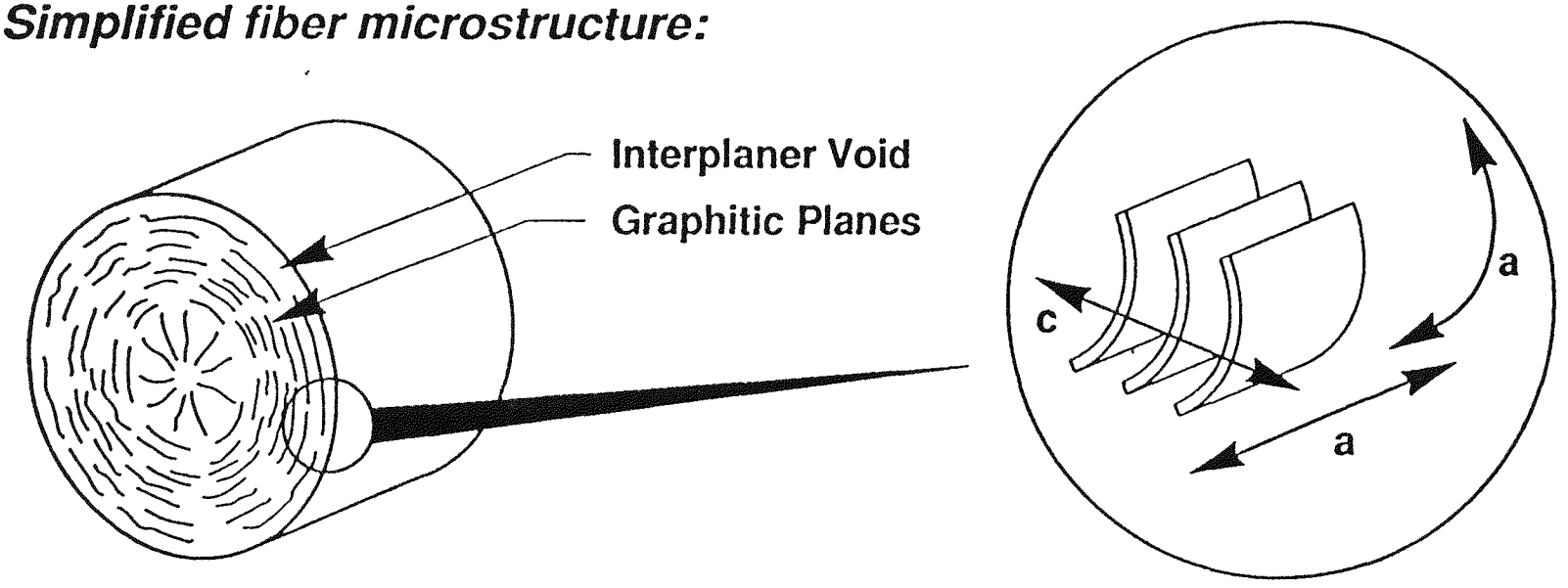

"Core-Sheath Model"

- *From single xtal graphite behavior we expect a-axis shrinkage and c-axis growth. However, Just as in the case of bulk graphites, c-axis growth is accomodated by interplaner voidage.*
- *Macroscopically we observe fiber axial shrinkage (Price et al, Gray) and fiber diameter shrinkage followed by swelling due to c-axis growth (Gray data).*

Figure 13. Schematic illustration of radiation damage in carbon fibers.

RADIATION DAMAGE IN CARBON FIBERS

- ***Amount of axial shrinkage and fluence at diametral turn around are functions of fiber structure, density, crystalinity and irradiation temperature.***
- ***Eventually diametral swelling will cause formation of cracks and voids within fiber.***

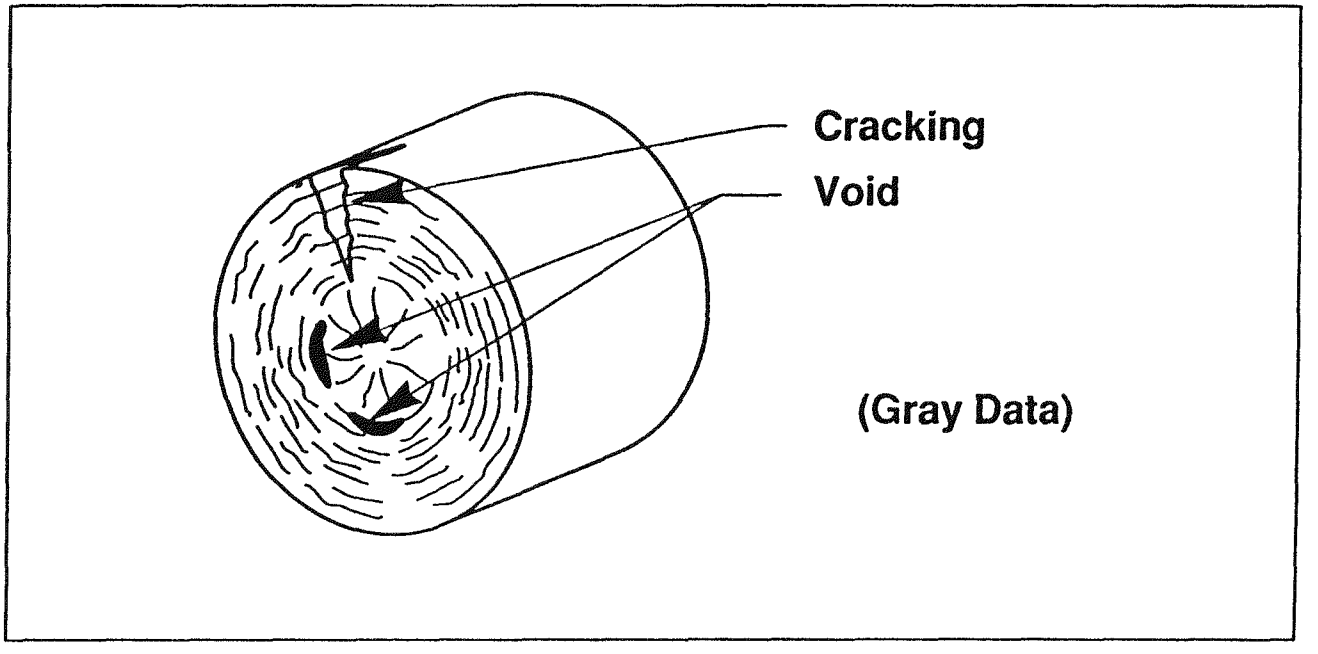

Figure 14. Schematic illustration showing development of irradiation induced fiber voids and cracks.

RADIATION DAMAGE IN C/C COMPOSITES

- *2D Cloths:* Fiber axial shrinkage will eliminate internal porosity (between bundles) and cause densification. (Gray Data)
- *2D Carbon - Carbon Composites.*

Parallel to cloth fiber shrinkage dominates.

Case I.

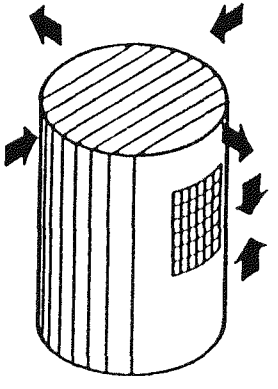

Cloth layers parallel to specimen axis (Mauny & Couve.)

Case II.

Radial Shrinkage

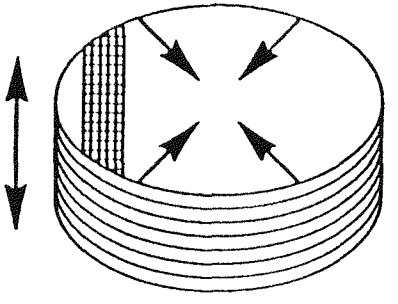

Cloth layers perpendicular to specimen axis (New data, Slagle & Hollenburg.)

Figure 15. Schematic illustration of irradiation induced dimensional changes in two-dimensional carbon-carbon composite specimens.